World Academy of Science, Engineering and Technology
International Journal of Mechanical and Materials Engineering
Vol:11, No:3, 2017

Robot Navigation and Localization Based on the Rat's Brain Signals

Endri Rama, Genci Capi, Shigenori Kawahara

***Abstract*—**The mobile robot ability to navigate autonomously in its environment is very important. Even though the advances in technology, robot self-localization and goal directed navigation in complex environments are still challenging tasks. In this article, we propose a novel method for robot navigation based on rat's brain signals (Local Field Potentials). It has been well known that rats accurately and rapidly navigate in a complex space by localizing themselves in reference to the surrounding environmental cues. As the first step to incorporate the rat's navigation strategy into the robot control, we analyzed the rats' strategies while it navigates in a multiple Y-maze, and recorded Local Field Potentials (LFPs) simultaneously from three brain regions. Next, we processed the LFPs, and the extracted features were used as an input in the artificial neural network to predict the rat's next location, especially in the decision-making moment, in Y-junctions. We developed an algorithm by which the robot learned to imitate the rat's decision-making by mapping the rat's brain signals into its own actions. Finally, the robot learned to integrate the internal states as well as external sensors in order to localize and navigate in the complex environment.

***Keywords*—**Brain machine interface, decision-making, local field potentials, mobile robot, navigation, neural network, rat, signal processing.

I. Introduction

NAVIGATION and localization are two closely linked processes with a great importance in everyday life. Navigation is a field of study that deals with moving objects from one place to another. In a broader sense, it can refer to any skill or study that involves trajectory determination and direction. One of the most important cognitive processes during navigation is decision-making, which requires the integration of many neural activities across different brain regions [1]. On the other hand, localization always involves the question "Where is the object now?" trying to find out the position relative to some landmark, usually the point of origin or destination [2]. These two processes are of a particular importance in robotics, and especially for mobile robots. The current location of a robot and the navigation strategies can be determined by using different sensors, depending on the characteristics of the mobile robot and the environment. Many researchers use different methods, such as: laser range finder and vision based navigation, joysticks and haptic devices, odometers, global positioning system (GPS), etc., for robot navigation [3]-[6]. However, the method accuracy depends on the type of robot and the specified environment. For example, one robot can localize itself and navigate very well in indoor environments, but it can fail and be useless in outdoor environments. In order to enhance these problems, scientist started to involve brain machine interface (BMI) for robot navigation and localization [7], [8].

BMI technologies are a class of neurotechnologies originally developed for medical assistive applications [9]. They are widely used for life improvement for people with clinical problems, paralyzed patients, as well as the direct control of prostheses and wheelchair robots [10]-[12]. However, the acquired signal quality is a very big problem for all BMI applications, depending on the electrode quality, location, signal power, etc. Generally the recorded signal is noisy; nevertheless, the tremendous growth of research in the field of neuroscience over the past decades offers an approach to address these limitations. Invasive-BMI technology is a method where the electrodes are implanted intracranially, directly to the desired animal's brain location, ensuring signals of the best quality [13]. Furthermore, it is well known that animals accurately and rapidly navigate in complex spaces. This ability to be organized in time and space stands on determining a heading direction [14], and localizing themselves in reference to the surrounding environmental cues. Therefore, animals utilize internal and external cues in navigating and constructing spatial representation [15]-[17]. However, few works simultaneously integrate the real rat's neuroscience data with robot navigation.

In this paper, we are focused on the investigation of the rat navigation and localization strategies, especially on the decision-making process, during a procedural maze task. Based on the previous behavior results, we suggested that rats might use two different navigation strategies to solve the complex Y-maze task [18], [19]. The theories presented in this paper are consistent with many other studies so far, which have demonstrated that hippocampus and striatum plays an important role on navigation and decision-making. In order to verify the proposed hypothesis, we recorded LFPs with bipolar electrodes implanted in these brain regions (two electrodes in Hippocampus Left-Right and one in Dorsolateral Striatum). The recorded LFPs are then analyzed and processed by using different MATLAB based toolboxes, in order to extract different features. These features are used as an input in the artificial neural network which is trained and used to control the robot.

This paper has the following structure. Section II explains materials and methods used for signal acquisition and processing. In Section III are presented the robot and the

E. Rama and Sh. Kawahara are with University of Toyama, Toyama, 930-855, Japan (email: endrirama@engineer.com, kawahara@eng.u-toyama.ac.jp).

G. Capi is with Hosei University, Tokyo, 184-8584, Japan (phone/fax: +81-042-387-6148; e-mail: capi@hosei.ac.jp).

artificial neural network used for robot control. The experimental results are summarized in Section IV. Section V concludes the paper.

II. Materials and Methods

All procedures were approved by the University of Toyama Committee on the Animal Care and were in accordance with the National Institutes of Health Guidelines for the Care and Use of Laboratory Animals.

A. Subjects

Two adult male Wistar/ST rats, purchased from Japan SLC, Inc. (Hamamatsu, Japan), served as subjects. Rats weighed between 290 g and 310 g at the time of arrival and were maintained individually in a controlled conditions room: room temperature 23 ± 2 ºC with a 12 hours light-dark cycle (lights on from 8:00 a. m.). Water was available ad libitum in the home cage. Food was restricted to motivate food seeking behavior and to maintain the rats at 85% of their free-feeding weights. A different cage is utilized to transport each rat from the housing room to the experiment area. In order to avoid the rat's confusion, the transportation cage is covered with a black curtain.

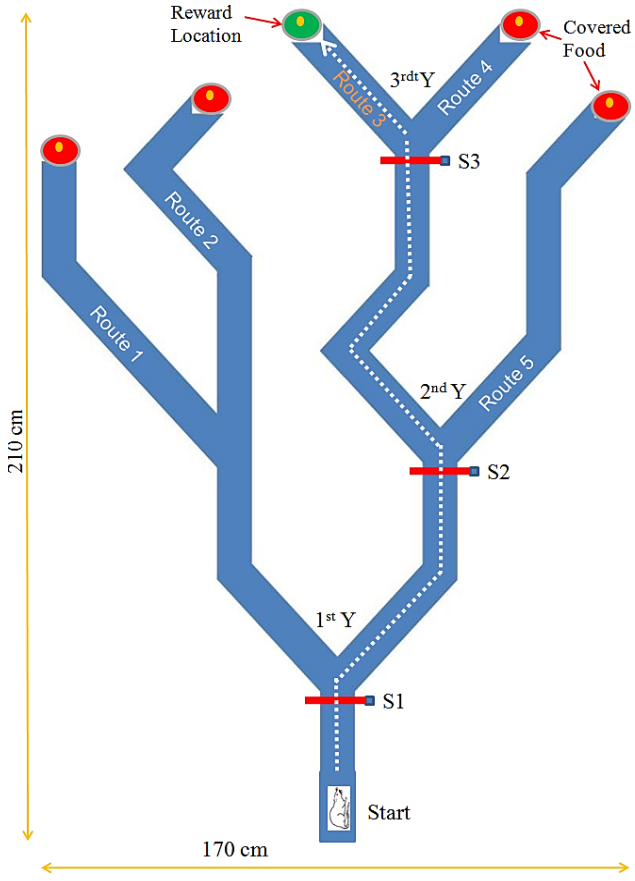

Fig. 1 Schematic representation of the multiple Y-maze apparatus

B. Apparatus

Animals were trained in a multiple Y-maze (170 cm x 210 cm), elevated 35 cm above the floor and consisted of one starting spot and five goal locations, as shown in Figs. 1 and 2. The goal arms (Routes) were numbered 1 to 5, clockwise. The maze was built of 10 cm width light blue polystyrene material and covered with a transparent PVC sheet. All the routes were surrounded by a 2 cm band in order to protect the animal from sliding and falling down.

At the end of each route a metallic cup of 2 cm depth is installed, which contains food (cereal pellets). The food odor was equal for each goal location. Four of them were covered with a metallic net, covered food, and one is left uncovered, the reward location. The experiment room is aspirated and kept at the constant temperature of 24±1 ºC. The environment was surrounded by heavy black curtains to acoustically isolate the Y-maze area and to avoid any light leaking from the outer environment, as shown in Fig. 2. Illumination was provided by two fluorescent bulbs. Hanging on each side of the experiment area are four different visually distinct cues: a square - at the home side, a triangle - at the goal location side, an X - on the left and a circle - on the right side of the maze.

As shown in Fig. 2, cues are printed in black, in 42 cm x 42 cm white cardboards. The same maze is used to perform the experiments with the mobile robot.

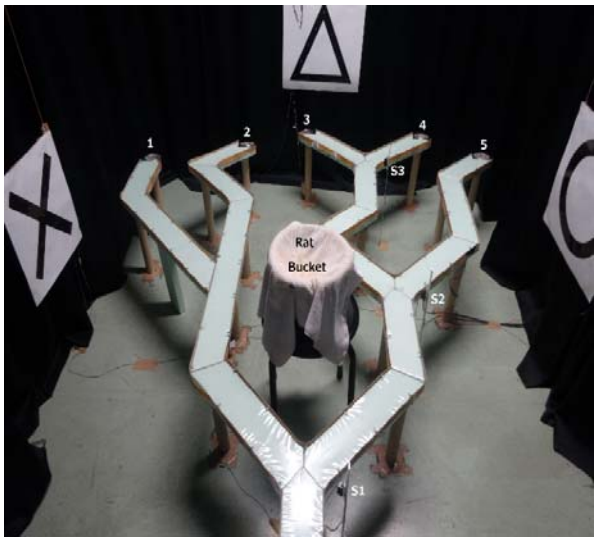

Fig. 2 Real experiment environment

C. Training Procedure

Firstly, the animal is trained to find the uncovered food location (the reward), to learn and memorize the correct route. During training, each rat was placed on the starting position and allowed to navigate freely on the maze environment until it reaches the reward location, which was fixed throughout the experiment. The training sessions, took place between 18:00 hrs to 20:00 hrs for all rats. Each rat received one session (20 trials) of training per day. For each training session, a correct trial was recorded only when the animal reached the reward on the first attempt, without making any incorrect turns on route to the Y junctions. A trial is terminated once the rat reaches the reward location. After the animal consumes the reward food, the experimenter relocates the rat to the bucket and cleans the maze. The rats were trained to learn the maze in a lighted

environment, until they reach an asymptotic level of learning and a criterion of at least 85% accuracy.

D. Data Acquisition

Surgery followed training and other experiments performed under different changes in the environment settings. We recorded LFP from hippocampus (left-right side) and dorsolateral striatum (left side), simultaneously. Three bipolar electrodes are implanted in the rat brain. The electrode positions are shown in Table I.

TABLE I
ELECTRODE POSITIONS

Animal	Coordinates			
	Brain Region	***AP***	***ML***	***DV***
Rat 1 & Rat 2	Hippocampus	- 4.92	± 2.5	-2.3
	Striatum	+ 0.96	- 3.6	-3.5

AP - anteroposterior axis, ML – mediolateral, DV - dorsoventral

After performing the perfusion and nissl stain process, we verified the real electrode location, as shown in Fig. 3. There are presented the 30 µm coronal sections around each electrode location, taken from Rat 1 brain.

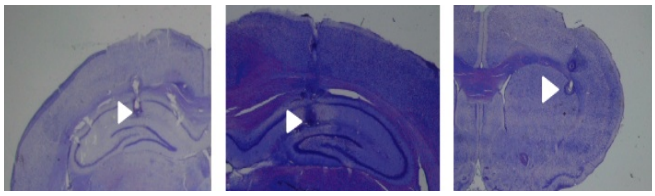

(a) (b) (c)

Fig. 3 Electrodes location in: (a) Hippocampus right side; (b) Hippocampus left side; (c) Dorsolateral Striatum left side

Electrodes pins on the animal head were connected with a pre-amplifier in order to eliminate the effect of noise on the recorded brain signals. LFPs are recorded by using a Nihon Kohden multichannel amplifier. The recording frequency was at 1 kHz and then LFPs are sub-sampled at 1 kHz for further analysis. All the data are stored as CSV file, in a personal computer.

In each Y-junction of the maze was installed a distance sensor (GP2Y0A21YK0F). Signals from these sensors are recorded together with LFPs in one channel, and are used to mark the rat position on the LFP data. Also, a video recording system (movement tracker) was used comprising of a low cost camera (KBRC-M05VU) and a Panasonic CF-N10 i5 notebook. The camera was fixed at the center of the experimental area, 170 cm above the maze, and had the following properties: 30 frames per second, infrared camera with self-adjustment of exposure and image adjustment functions. An easy MATLAB-based GUI was built in order to track the rat movement, to collect the camera data and to calculate the time spent by the animal to reach the reward location. Fig. 4 shows the Rat 2 movement tracked in three different sessions.

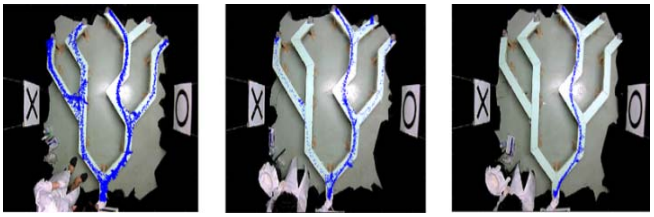

(a) (b) (c)

Fig. 4 Rat movement tracked from the camera in three different sessions: (a) in the initial phase of training; (b) rat almost learned the task; (c) rat passed the 85% correct learning criteria

E. Feature Extraction

LFPs are generated by neuronal ensembles and contain information about the underlying cellular activity. They have extensively been used to investigate central circuit functions. The recorded data are processed offline by using MATLAB signal processing toolbox and Chronux toolbox, in order to extract different features. Fig. 5 represents raw Hippocampal and Striatal LFP traces recorded simultaneously during a single representative trial (Rat 1, Session 3, Trial 5).

The recorded data are represented by matrix $S \in R^{(C \times N)}$ where C is the number of channels (Sensor, HPC_L, HPC_R, and STR_L) and N is the number of sample time points.

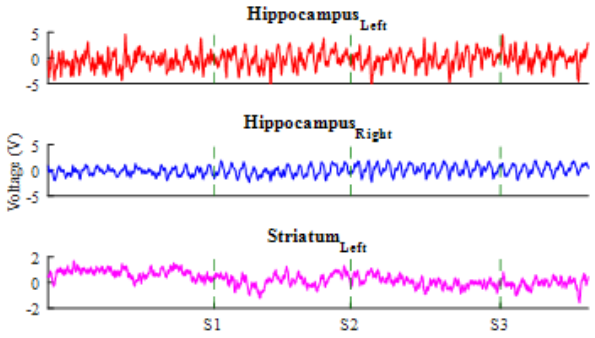

Fig. 5 Raw LFP trace recorded during a single representative trial

In these LFP traces, the researchers focused on the decision-making events, represented by sensors S1, S2 and S3. These markers represent the moment in which the animal starts turning left or right at each Y-junction, so the animal has already decided which route to follow. The one second time window at the Y-junction, 0.5 seconds before and after the event, was analyzed as shown in Fig. 6. For every window in each LFP trace, the Fast Fourier Transformation (FFT) was performed using (1):

$$X(\omega) = \int_{-\infty}^{\infty} x(t)\, e^{-i\omega t} dt \qquad (1)$$

We obtained the frequency representation and the power spectra of the processed LFPs. The average value of each feature for all sessions and animals is then calculated. The data are stored in a feature vector $F(f_i)_{(N \times C) \times 1}$, where fi are all features extracted from the Hippocampal and striatal LFPs. These features are used to train a feed forward neural network.

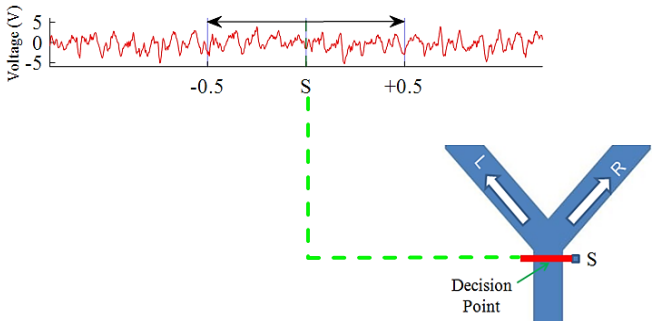

Fig. 6 Time windows around decision-making events, to conduct the subsequent analysis

III. Robot and Artificial Neural Network

In this section, the architecture of the neural network used to control the robot and the robot characteristics is defined. Based on the input data, the e-puck robot motion is determined and sent by a Bluetooth connection with a MATLAB-based personal computer.

A. E-puck Robot

All the conducted experiments in this work use an e-Puck robot, as seen in Fig. 7. This robot was selected for its simple mechanical structure and fine electronics design, offering many possibilities with its sensors, processing power and extensions. E-puck is small, flexible and user-friendly, and has good robustness. It does not need any cables, providing optimal working comfort [20], [21].

Fig. 7 E-puck Robot

The e-puck robot has several sensors, including: sound sensors, encoders, odometry sensors, camera, proximity sensors, etc. In our experiments, the robot utilizes the data from proximity sensors to perceive the decision-making moment in the Y-junctions, as shown in Fig. 8. A threshold value (around 2.3 cm) for the sensor IR2 was set, so that when this threshold is passed the robot stops moving. Moreover, encoder sensors are used by the robot during the navigation in other parts of the maze, especially to define the moment when the robot reaches the reward location.

B. Neural Network

The decision-making process, based on the animal's LFPs, is determined by applying a feedforward neural network (FFNN), as shown in Fig. 9.

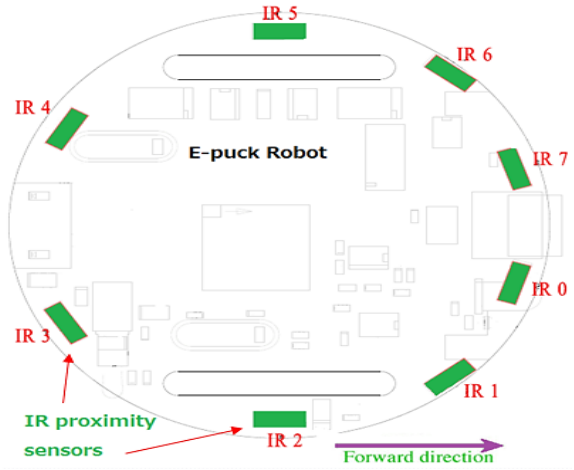

Fig. 8 E-puck robot proximity sensors

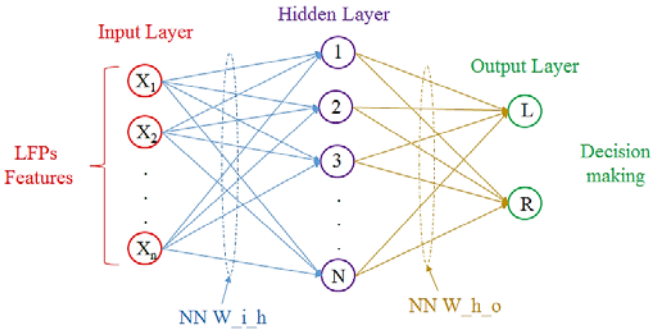

Fig. 9 Artificial neural network architecture

Three neural networks were employed, one per each Y-junction, with six inputs - eight hidden and two output units. Six features, two from each LFP, are used as an input to the neural network. In the implemented neural networks, the sigmoid function is used as an activation function for the hidden and output units, as shown in (2):

$$y(i) = \frac{1}{1+e^{-x(i)}} \tag{2}$$

where:

$$x(i) = \sum w(j,i) * y(j) \tag{3}$$

$w(j,i)$ are weights connections between nodes of different layers.

Two output units of the neural controllers are the decision-making values "0" or "1", which represents:

1. Output [0,1] – robot will turn right;
2. Output [1,0] – robot will turn left.

The value of the output neurons is not exactly "0" or "1", but varies in the range [0,1]. In our implementation, the output is 1 if the value is above the threshold 0.9, and 0 for other values. In order to generate the best solution for the decision-making task, a floating point Genetic Algorithm (GA) was used.

IV. Results

A. Selected Features from Hippocampal and Striatal LFPs

Firstly, we pre-processed all the recorded LFP data and removed the bad data. As described above, the focus was on the decision-making process and the analysis of the one second time window LFP data in each Y-junction, 0.5 seconds before and after the event. In this paper, we considered the cases when the rat made a correct and/or a wrong choice. The average value of each feature for all sessions and then for all animals is calculated. As shown in Figs. 10-12, we found a dominant Theta (7-11 Hz) and Beta (15-20 Hz) range oscillations in hippocampal LFP, in all Y-junctions, and for correct and wrong choices. On the other hand, no dominance of theta or beta oscillation was found in the dorsolateral striatum, except in the case when the animal performed a wrong choice, and a boost in theta oscillation was recorded.

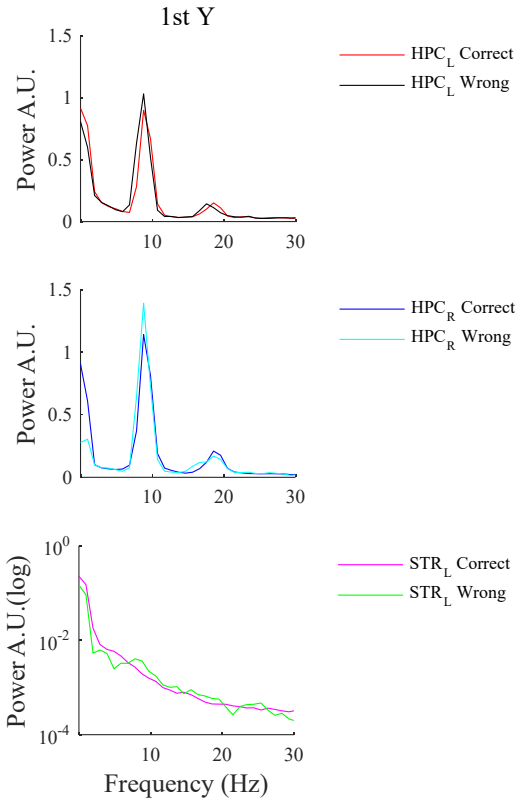

Fig. 10 Representations of hippocampal and striatal power for correct and wrong choices in the 1st Y-junction

There were marked contrasts between the left and right hippocampal LFPs power in all the Y-junctions, for correct and wrong choices. Along with this, during the decision-making epoch in the 1st and 2nd Y-junctions of the maze, the peak frequency of the hippocampal beta oscillation significantly changed from 17.58 Hz to 18.55 Hz for the correct and wrong choices. In our implementation, for each recording site: HPC_L, HPC_R, and STR_L, we selected the peak frequency value and the power value of theta oscillation for correct choices, as an input for the neural network.

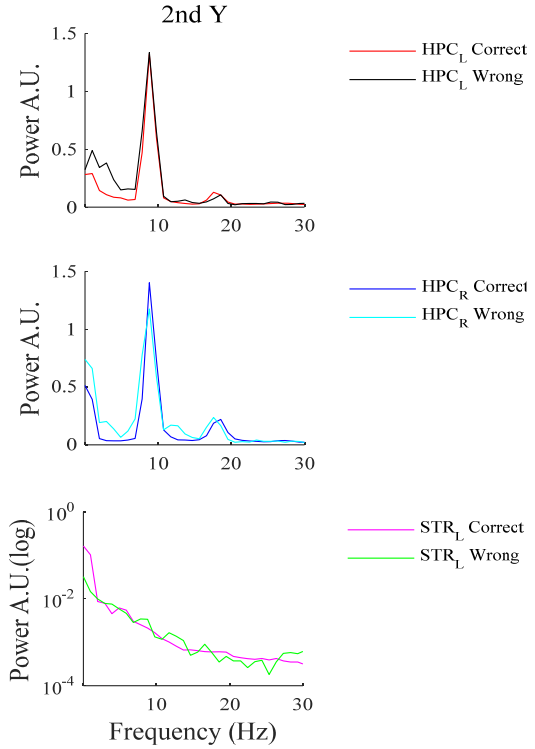

Fig. 11 Representations of hippocampal and striatal power for correct and wrong choices in the 2nd Y-junction

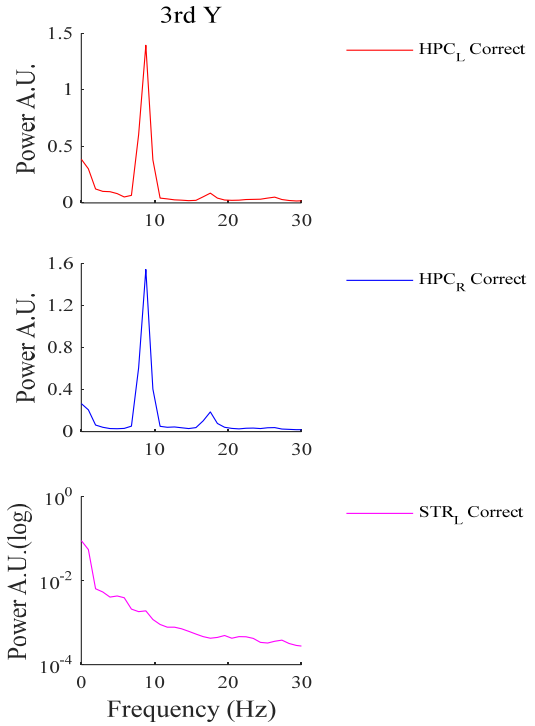

Fig. 12 Representations of hippocampal and striatal power for correct choice in the 3rd Y-junction

B. Robot Navigation

The offline trained FFNN with the extracted LFP features, is used to control the robot during the decision-making process. Fig. 13 shows the robot motion during an experiment trial

where the robot reached the reward location after three accurately made decisions by the neural controller in the Y-junctions.

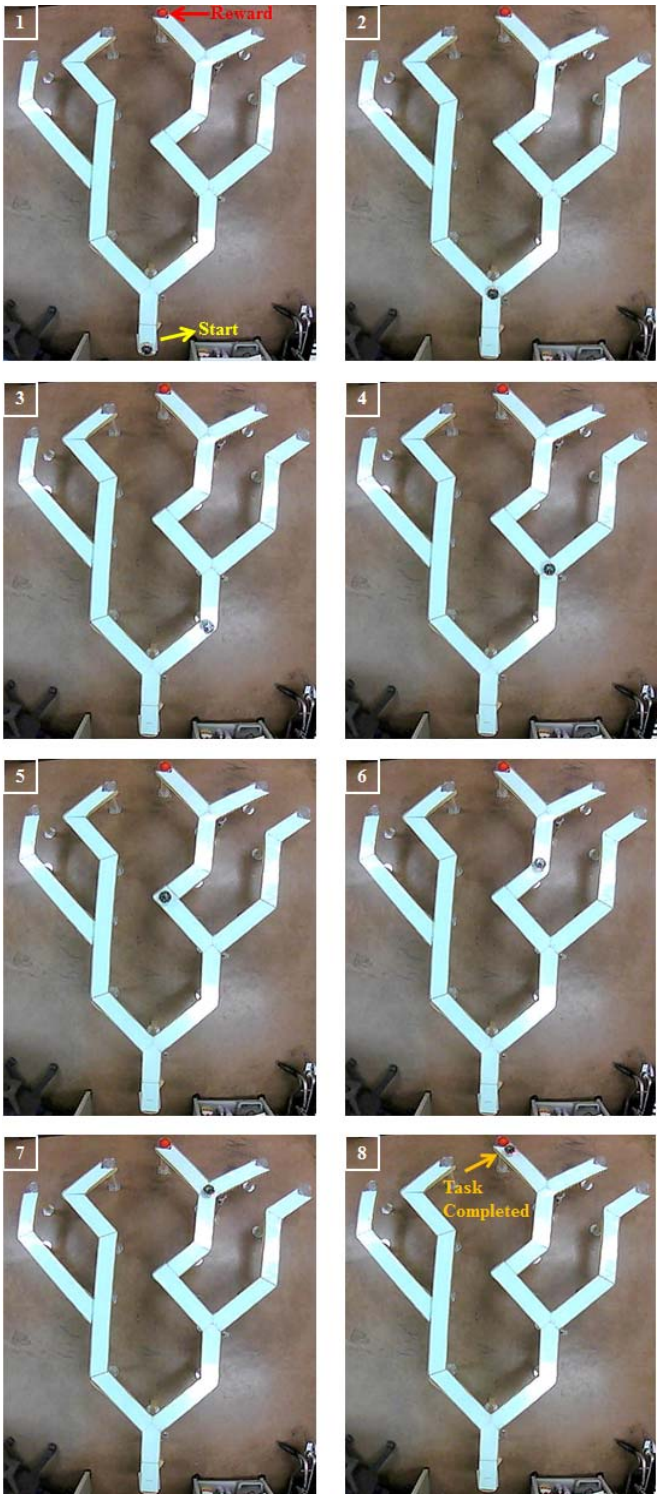

Fig. 13 Robot decision-making and motion during one experiment trial

Fig. 13.1 shows the robot in the start position, ready to move forward. The robot detects the 1st Y-junction using its sensors and stops moving, as shown in Fig. 13.2. Neural Network 1 takes the decision to turn right, and the robot turns right and moves forward. Fig. 13.3 shows the robot position in the maze, navigating toward the reward location. The robot then detects the 2nd Y-junction by its proximity sensors and stops moving forward, as shown in Fig. 13.4. Neural Network 2 takes the decision to turn left. The robot turns left and moves forward toward the next Y-junction, as shown in Figs. 13.5 and 13.6. When the robot reaches the 3rd Y-junction, Neural Network 3 takes the decision to turn left. It turns left and moves toward the reward location, as in Fig. 13.7. Fig. 13.8 shows the task completed by the robot, which reached the reward location by using the animal LFPs features and its own external sensors.

V. Conclusions

This paper presents a novel method for robot navigation and localization based on an animal's brain activity. The data presented above shows some distinctive features on the hippocampal and striatal LFPs during the animal's decision-making process. In addition, this work shows that we can use these features to control the robot to perform the same decisions as animals do.

A distinctive feature of this study is the usage of the real neural network, the animal brain, and artificial intelligence. The results clearly show how the robot learned to integrate the internal states, as well as external sensors, in order to localize and navigate in the complex environment. Furthermore, the results also show fast and robust robot localization. The authors are working to develop an algorithm that can be easily modified for different types of robots and environments.

References

[1] B. Hofmann-Wellenhof, K. Legat, M. Wieser, *Navigation: Principles of Positioning and Guidance*, Springer-Verlag Wien, 2003, pp. 5–6.
[2] H. Yussof, "*Robot Localization and Map Building*", Publisher: InTech, March 2010, Edited Volume, Ch. 7, pp. 133-151.
[3] G. Capi, M. Kitani, K. Ueki, "Guide robot intelligent navigation in urban environments," in *Advanced Robotics*, Volume 28, Issue 15, pp. 1043-1053, 2014.
[4] G. Capi, "A Vision based Approach for Intelligent Robot Navigation," in *International Journal of Intelligent Systems Technologies and Applications (IJISTA)*, Vol. 9, No. 2, July 2010.
[5] B. Hua, E. Rama and G. Capi, "A human-like robot intelligent navigation in dynamic indoor environments," presented at the 2nd IEEJ International Workshop on Sensing, Actuation, Motion Control, and Optimization (SAMCON2016), March 7-8, 2016, Tokyo, Japan.
[6] T. Oshima, M. Li, E. Rama and G. Capi, "Intelligent robot navigation for surveillance behavior - a remote based approach," presented at the 2nd IEEJ International Workshop on Sensing, Actuation, Motion Control, and Optimization (SAMCON2016), March 7-8, 2016, Tokyo, Japan.
[7] M. Mano, G. Capi, "An adaptive BMI based method for real time wheelchair navigation," in *International Journal of Innovative Computing, Information and Control (IJICIC)*, Vol. 9, No. 12, pp. 4963-4972, 2013.
[8] G. Capi, "Real robots controlled by brain signals—A BMI approach," in *International Journal of Advance Intelligence*, Vol.2, pp. 25–35, 2010.
[9] N. Birbaumer et al. (1999), "A spelling device for the paralyzed," in *Nature*, Vol. 398, pp.297–298.
[10] F. Piccioneet et al. (2006), "P300-based brain computer interface: reliability and performance in healthy and paralyzed participants," in *Clinical Neurophysiology*, Vol. 117, pp. 531–537.
[11] B. J. Lance, S. E. Kerick, A. J. Ries, K.S. Oie, K. McDowell, "Brain–Computer Interface Technologies in the Coming Decades" in *Proceedings of the IEEE*, vol.100, pp.1585-1599, May 2012.
[12] S. Halder, D. Agorastos, R. Veit, E.M. Hammer, S. Lee, B. Varkuti, M.

Bogdan, W. Rosenstiel, N. Birbaumer, A. Kübler, "Neural mechanisms of brain–computer interface control," in *NeuroImage*, Vol. 55, pp. 1779–1790, 2011.
[13] M. A. Lebedev and M. A.L. Nicolelis, "Brain–machine interfaces: past, present and future", in *TRENDS in Neurosciences*, Vol.29 No.9, pp. 536-546, July 2006.
[14] C. R. Gallistel, "*The organization of learning*," Cambridge: MA: Bradford/MIT Press, 1990.
[15] A. S. Etienne, R. Maurer, J. Berlie, B. Reverdin, T. Rowe, J. Georgakopoulos, V. Seguinot, "Navigation through vector addition," in *Nature*, Vol. 396, pp. 161-164, 1998.
[16] A. S. Etienne, R. Maurer, V. Seguinot, "Path integration in mammals and its interactions with visual landmarks," in *Journal of Exp. Bio*., Vol. 199, pp. 201-209, 1996.
[17] S. J. Shettleworth, "*Cognition, evolution, and behavior*," New-York: Oxford University Press, 1998.
[18] E. Rama, G. Capi, S. Mizusaki, N. Tanaka, S. Kawahara, "Effects of Environment Changes on Rat`s Learned Behavior in an Elevated Y-Maze," in *Journal of Medical and Bioengineering*, Vol. 5, No. 2, pp. 113-118, April 2016.
[19] E. Rama, G. Capi, N. Tanaka, S. Kawahara, "Rat`s Spatial Learning in an Novel Elevated Y-Maze," presented at the 5th Annual International Conferences on CBP 2016, February 2016, Singapore.
[20] F. Mondada, M. Bonani, X. Raemy, J. Pugh, C. Cianci, A. Klaptocz, S. Magnenat, J. C. Zufferey, D. Floreano, A. Martinoli, "The e-puck, a Robot Designed for Education in Engineering," in *Proceedings of the 9th Conference on Autonomous Robot Systems and Competitions*, Vol. 1(1), pp. 59-65, 2009.
[21] J. Hubert, Y. Weibel, "*ePic2*", Documentation, November 2008.